Rare Metal Materials and Engineering
Volume 47, Suppl. 2, August 2018
Cite this article as: Rare Metal Materials and Engineering, 2018, 47(S2): 250-253.

Preparation and Characterization of $LiInO_2$ Nanoparticles (NPs) by a Sol-gel Method

Zhang Xiangchao[1], Huang Duan[1,2], Liu Fang[1,2], Xu Kaiqiang[1,2], Zhang Shiying[1]

[1] Hunan Key Laboratory of Applied Environmental Photocatalysis, Changsha University, Changsha 410022, China; [2] Hunan University, Changsha 410082, China

Abstract: $LiInO_2$ nanoparticles (NPs) have been synthesized by a sol-gel method. The structure of the as-synthesized $LiInO_2$ NPs were characterized using X-ray diffraction analysis (XRD), scanning electron microscopy (SEM), and ultraviolet-visible (UV-vis) analysis technique. The photocatalytic performances of samples were evaluated using the methyl blue (MB) as a model dye pollutant. Additionally, the photocatalytic degradation mechanism for MB of the $LiInO_2$ NPs were also proposed. The results show that the as-prepared $LiInO_2$ presents a $LiFeO_2$ structure with the uniform size about 50~100 nm. The calcination temperature can severely impact the structure and photocatalytic performance of the $LiInO_2$ NPs. The degradation rate of MB is 92% under simulated sunlight using 300 W xenon lamp for 90 min. The trapping experiments of the reactive species show that the holes play an important role in the process of the MB degradation. The results obtained from this work suggest that the $LiInO_2$ NPs will have potential applications in wastewater treatment.

Key words: $LiInO_2$; photocatalytic activity; nanoparticles (NPs); methyl blue (MB); sol-gel

Nowadays, with the development of industry, the environmental contamination caused by organic pollutants is becoming a growing problem globally. Semiconductor photocatalysis, as a green chemistry technique, appears to be one of the most efficient techniques for the organic pollution in water environment since the report about TiO_2 photocatalysis [1]. Photocatalysis can completely degrade organic pollutants into harmless inorganic species such as CO_2, H_2O and mineral acids (without the secondary contamination) at room temperature and ambient pressure. However, traditional TiO_2 NPs are still restricted by its wide band gap and rapid recombination of photogenerated electron-hole pairs[2,3]. Therefore, the development of the advanced photocatalysts has become one of the up-to-date active research areas around the world.

Recently, Indium-containing photocatalysts have attracted more attention in the field of solar energy conversion and environment remediation due to their high catalytic activities under visible light[4]. Particularly, ternary oxides semiconductor with the general formula $A^{+1}B^{+3}O_2$ based on the mineral delafossite ($CuFeO_2$) present great photocatalytic applications due to their stability and interesting electronic structures[5]. Among them, $NaInO_2$ has already demonstrated to be one of the candidates for organic pollutants degradation and water splitting. Lithium-indium oxide ($LiInO_2$ has a similar crystal structure with $NaInO_2$) has attracted much attention due to its wide applications on solid-state scintillators, luminescent materials, energy storage and conversion devices [6]. However, to the best of our knowledge, the photocatalytic performance of $LiInO_2$ NPs is barely reported.

Based on the above considerations, in this work, we prepared $LiInO_2$ NPs by a sol-gel method. The structure of the synthesized $LiInO_2$ NPs was characterized using X-ray diffraction analysis (XRD), scanning electron microscopy (SEM), and ultraviolet-visible (UV-vis) analysis. The photocatalytic performances of samples were evaluated using the methyl blue (MB) as a model dye pollutant. Additionally, the mechanism of photocatalytic degradation MB of the $LiInO_2$ NPs was also proposed.

1 Experiment

All reagents were of analytical grade and used without further purification or treatment. $LiInO_2$ NPs were synthesized by the sol-gel method. In a typical procedure, 0.02 mol $In(NO_3)_3$ $9H_2O$ and 0.02 mol $LiNO_3$ were dissolved in 60 ml ethylene alcohol

Received date: July 30, 2017
Foundation item: National Natural Science Foundation of China (51272032); Natural Science Foundation of Hunan Provincial of China (2016JJ6008); Scientific Research Fund of Hunan Provincial Education Department (17B029)
Corresponding author: Zhang Shiying, Ph. D., Professor, Hunan Key Laboratory of Applied Environmental Photocatalysis, Changsha University, Changsha 410022, P. R. China, Tel: 0086-731-84261297, E-mail: cdzhangshiying@163.com

(C_2H_6O, EtOH). The mixed solution was magnetically stirred for 5 h at 60~70 ℃ to form yellow gel. The gel was further treated at 150 ℃ for 12 h, before being sintered at 500~900 ℃ for 2 h to obtain $LiInO_2$ NPs. The samples were named as T500, T600, T700, T800 and T900.

Structural features and phase composition of the samples were determined using Bruker AXS D8 Advance X-ray diffractometer with Cu-Kα radiation (λ=0.154 06 nm). The surface morphology of as-prepared samples were observed using a scanning electron microscope (SEM JEOL Model JSM-6360LV). The ultraviolet-visible (UV-vis) absorption spectra were acquired by UV-vis spectrometer (UV-2450, Shimadzu).

The photocatalytic activity of the prepared samples under visible light was estimated by measuring the degradation rate of methylene blue (MB) in an aqueous solution [7]. The photocatalyst (0.05 g) was dispersed in 50 mL of MB solution (6.25 mg/L) in an 8 cm diameter culture dish. The mixed solution was kept in the dark for 1 h to reach adsorption–desorption equilibrium for MB molecules on the photocatalysts. Finally, a 300 W xenon lamp (Shanghai Lansheng Electronic Co., China) was used as a simulated sunlight source, which was located approximately 25 cm above the culture dish. At 0, 10, 20, 30, 40, 50, 60, and 90 min, 3 mL of the upper MB solution was sampled, and detected at 664 nm by the UV−Vis spectrometer (UV-721). The photocatalytic activity was calculated using C_t/C_0, where C_0 and C_t are the MB concentrations (mg/l) at initial state and after irradiation for t min, respectively. To determine the dominant reactive species, radical scavenging experiments were performed with the same procedure except that scavengers were added into MB solution.

2 Results and Discussion

2.1 Microstructure of $LiInO_2$ NPs

Fig.1 shows XRD patterns of $LiInO_2$ NPs synthesized by a sol-gel method with different calcination temperatures range from 500 ℃ to 900 ℃. The pattern after calcination at 500 ℃ shows all diffraction peaks match very well with the JCPDS (06-0416) standard data of In_2O_3. The diffraction pattern for crystalline $LiInO_2$ NPs are present with an orthorhombic structure at 600 ℃ and no impurity phase is found, indicating the obtained samples with single phase of $LiInO_2$. The diffraction patterns for the samples have major diffraction peaks at 22.68 °, 35.12 °, 35.63 °, 38.52 °, 41.87 °, 48.14 °, 53.40 °, 56.03 °, and 58.16 °, corresponding to (101), (112), (103), (004), (200), (211), (105), (213), and (204) lattice planes of $LiInO_2$ (JPCDS No. 89-3853), respectively. Interestingly, the increasing calcination temperatures result in an increase in the intensity and sharpness of the diffraction peaks. This trend is clearly indicative of an improvement in the degree of crystallinity corresponding to the formation of larger particles with fewer defects.

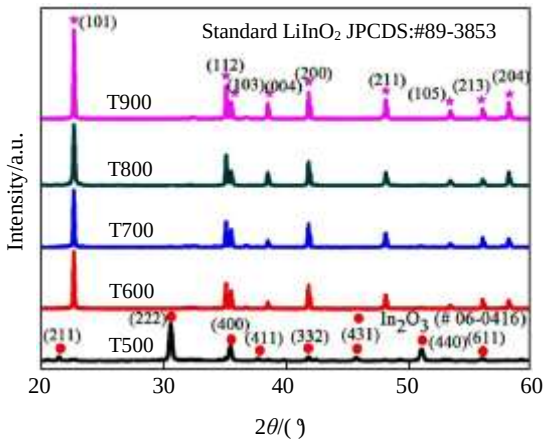

Fig.1 XRD patterns of $LiInO_2$ NPs synthesized by sol-gel method with different calcination temperatures

The morphologies and microstructures of $LiInO_2$ NPs were observed by scanning electron microscopy (SEM). As can be seen in Fig.2, a typical aggregated irregular morphology with an average particle size of 50~100 nm can be found for the T600 sample. The crystallite sizes of $LiInO_2$ have grown bigger with the calcination temperature increasing, which is consistent with the results in XRD.

The optical property of samples was investigated using UV-vis diffuse reflectance spectra (DRS) and the band gap was estimated from the absorption onset[8]. As shown in Fig.3a, the absorption edge of $LiInO_2$ is located at approximately 350 nm and displays absorption in the UV light regions, which is in accordance with the band gap absorption reported in previous study[9]. However, careful observation reveals that T800 and T900 samples exhibit intensive optical responses compared to T600 sample, which might be ascribed to the nano-sized effects. Furthermore, based on the theory of optical absorption for indirect band gap semiconductors, the band gap

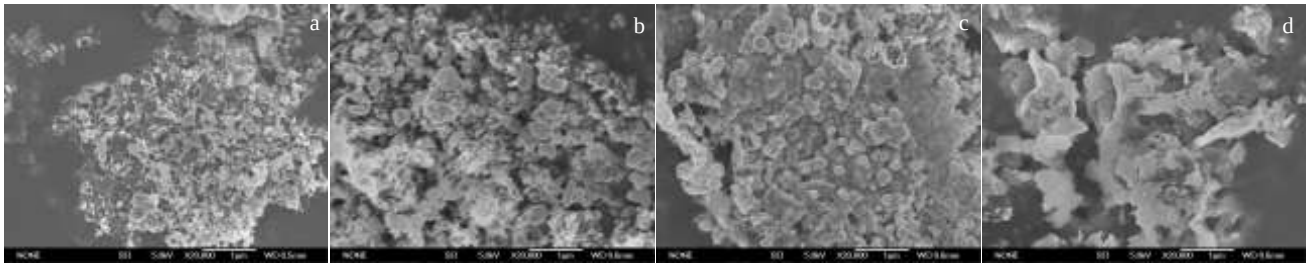

Fig.2 SEM images of $LiInO_2$ NPs synthesized by sol-gel method with different calcination temperatures: (a) T600, (b) T700, (c) T800, and (d) T900

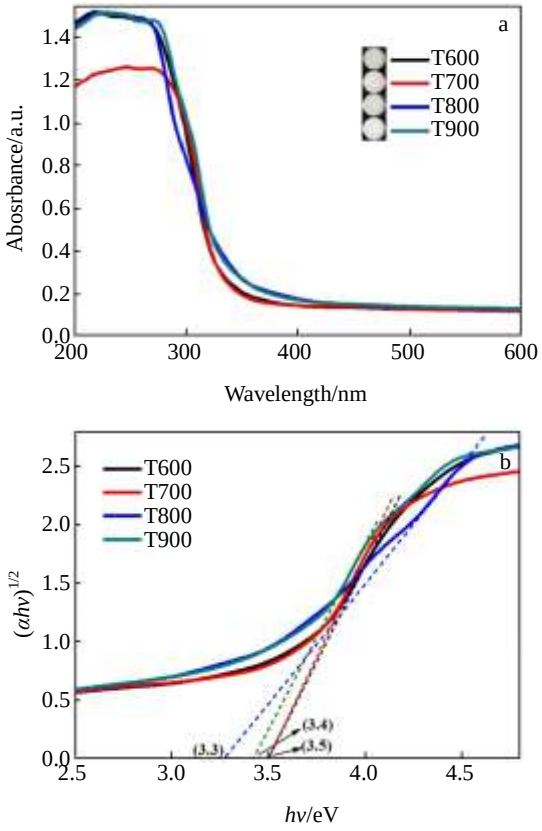

Fig.3 UV-vis absorption spectra of $LiInO_2$ NPs (a) and the calculated band gaps of $LiInO_2$ NPs based on the relationship of $(\alpha hv)^{1/2}$ and hv (b)

energy of the as-prepared samples can be calculated with the following equation[5]: $\alpha hv = A(hv-E_g)^2$, where α, hv, A and E_g are the absorption coefficient, photon energy, a constant and band gap, respectively. As a consequence, according to above equation, the energy band gaps of T600, T700, T800 and T900 samples from the plots of $(\alpha hv)^{1/2}$ versus photon energy hv are estimated to be about 3.5 eV, 3.5 eV, 3.3 eV, and 3.4 eV, respectively.

2.2 Photocatalytic performance of $LiInO_2$ NPs

The photocatalytic activity of the as-prepared $LiInO_2$ NPs were evaluated by the degradation of MB dye under simulated sunlight using 300 W xenon lamp. The degradation rates of MB dye over different photocatalysts are shown in Fig.4. It can be seen that the degradation rate of the commercialized P25 catalysts is about 39.86%, suggesting a certain photo-degradation. While in the case of the $LiInO_2$ samples under the similar experimental conditions, the photocatalytic activity of $LiInO_2$ NPs for degradation followed the order of T800 > T700>T600>T900. Interestingly, it can be seen that the highest photocatalytic performance of the T800 sample is enhanced by 52.36% comparing to that of the P25 sample. On the other hand, from the compared digital photos about the MB solution at initial state and final state, the color of the

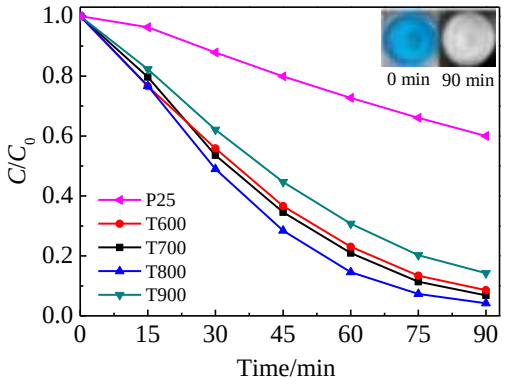

Fig.4 Photocatalytic performance of $LiInO_2$ NPs for degradation MB (the inset is digital photos of the MB solution at initial state t=0 min and final state t=90 min)

suspension has changed from blue to colorless finally. These results indicate that the prepared $LiInO_2$ NPs as an efficient photocatalyst may have a broad potential application in the field of the wastewater treatment.

To further investigate the photocatalytic mechanism, triethanolamine (TEOA, 0.01 mol/L), isopropanol (IPA, 0.02 mol/L) and p-benzoquinone (BZQ, 0.001 mol/L) are employed as scavengers for photogenerated holes (h^+), hydroxyl radicals (OH) and superoxide anion radicals (O^{2-}), respectively [10]. As shown in Fig.5, the degradation efficiency of $LiInO_2$ is unchanged for IPA and BZQ introduction, while decreased through introducing TEOA into MB solution. The results indicate that only photogenerated holes predominate the photocatalytic reaction of $LiInO_2$ [11-15].

Based on the experiment results, an electron transfer model is proposed to better understand the photocatalytic mechanism (Fig.6). $LiInO_2$, a large band gap, can be excited by simulated sunlight to isolate excitation electrons and photogenerated holes. The reactive specie trapping experiments show that the holes play an important role in MB photo-degradation. The MB molecules are absorbed on the $LiInO_2$ surface and degraded into oxidation products by photogenerated holes.

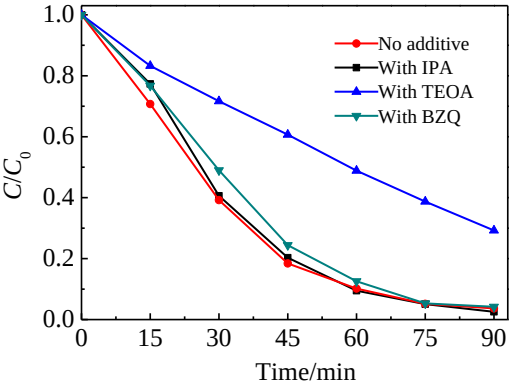

Fig.5 Effects of various trapping agents on degradation of MB

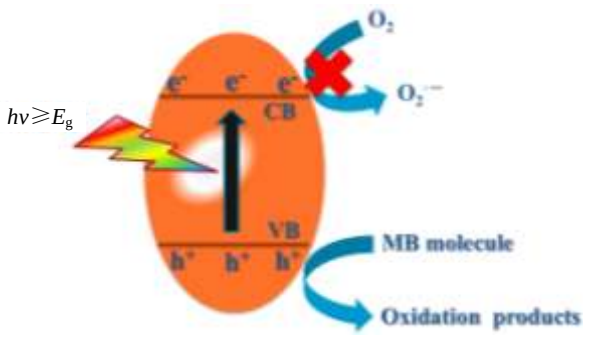

Fig.6 Catalytic mechanism of $LiInO_2$ NPs for MB photo-degradation under simulated sunlight

3 Conclusions

1) $LiInO_2$ NPs can be prepared by a sol-gel method.

2) The as-synthesized $LiInO_2$ NP has an orthorhombic structure with the uniform size about 50~100 nm.

3) The degradation rate of MB is 92.22% under simulated sunlight using 300 W xenon lamp for 90 min.

References

1 Fujishima A, Honda A. *Nature*[J], 1972, 238: 37

2 Li X, Yu J G, Mietek J. *Chemical Society Reviews*[J], 2016, 45: 2603

3 Tang A D, Jia Y R, Zhang S Y *et al*. *Catalysis Communications*[J], 2014, 50: 1

4 Kawakami S, Sasaki M, Tabata H *et al*. *Journal of Alloys and Compounds*[J], 2003, 359: 278

5 Hsiao Y J, Chang S C. *Materials Letters*[J], 2011, 65: 2920

6 Kushida K, Kuriyama K. *Physica Status Solidi (C)*[J], 2016, 3(8): 2800

7 Huang D, Zhang S Y, Zhang X C *et al*. *The Journal of Chinese Ceramic Society* [J], 2016, 44(7): 2019

8 Zhang X C, Luo Z, Wang Y T *et al*. *Chemistry Letters*[J], 2016, 45(10): 160709

9 Lekse J W, Haycock B J, Lewis J P *et al*. *Journal of Materials Chemistry A*[J], 2014, 24(24): 9331

10 Xu K, Xu D F, Zhang X C *et al*. *Applied Surface Science*[J], 2017, 391: 645

11 Liang Y, Wang H, Liu L *et al*. *Rare Metal Materials and Engineering*[J], 2015, 44(5): 1088

12 Zhou G H, Ding H Y, Zhu Y F *et al*. *Rare Metal Materials and Engineering*[J], 2016, 45(5): 1117

13 Zhang Y J, Kang L, Liu L C. *Rare Metal Materials and Engineering*[J], 2015, 44(12): 3032

14 Zhang X C, Xu D F, Jia Y R *et al*. *RSC Advance*[J], 2017, 7: 30392

15 Zhang X C, Xu D F, Huang D *et al*. *Journal of American Ceramic Society*[J], 2017, 100(7): 2781

纳米 $LiInO_2$ 光催化剂的溶胶-凝胶法制备与表征

张向超[1]，黄　锻[1,2]，刘　芳[1,2]，许凯强[1,2]，张世英[1]

(1. 长沙学院 环境光催化应用技术湖南省重点实验室，湖南 长沙 410022)

(2. 湖南大学，湖南 长沙 410082)

摘　要：利用溶胶-凝胶法制备了 $LiInO_2$ 纳米材料，采用 X 射线衍射(XRD)、扫描电镜(SEM)和紫外-可见吸收光谱等测试手段，研究了制备条件对 $LiInO_2$ 微观结构的影响，并以亚甲基蓝为目标降解物研究了 $LiInO_2$ 的光催化性能。结果表明：制备的 $LiInO_2$ 纳米粒子具有 $LiFeO_2$ 的晶型，颗粒尺寸 50~100 nm，制备样品的焙烧温度对其结构和性能产生了明显地影响，在氙灯(300 W)照射 90 min 条件下，纳米 $LiInO_2$ 对亚甲基蓝的光催化降解率达 92%，活性位点捕获实验表明光生空穴在降解亚甲基蓝的机制中占主导作用。

关键词：$LiInO_2$；光催化；纳米材料；亚甲基蓝；溶胶-凝胶

作者简介：张向超，男，1979 年生，博士，副教授，长沙学院环境光催化应用技术湖南省重点实验室，湖南 长沙 410022，电话：0731-82461297，E-mail: xczhang@ccsu.edu.cn